International Journal of Thermophysics, Vol. 19, No. 1, 1998

Experimental Measurements of the Speed of Sound in *n*-Hexane from 293 to 373 K and up to 150 MPa

J. L. Daridon,[1,2] B. Lagourette,[1] and J.-P. E. Grolier[3]

Received September 16, 1997

Speed-of-sound measurements were performed at pressures up to 150 MPa in the temperature range from 293 to 373 K on *n*-hexane in the liquid state. Theses data were then used to evaluate the isentropic and isothermal compressibility in the same range of pressures and temperatures. The speed-of-sound measurements, as well as the related compressibility coefficients, compare very well with the values calculated from the correlation of Randzio et al. Volumetric properties also compare very well with the direct measurements reported in the standard reference data tables.

KEY WORDS: compressibility; hexane; pressure; speed-of-sound; ultrasonic velocity.

1. INTRODUCTION

The thermophysical properties of pure substances in the liquid state as functions of temperature and pressure are of great interest not only for industrial applications (for example, in the oil and gas industry), but also for fundamental aspects in view of developing models for an accurate representation of dense fluids. If literature data are generally consistent at atmospheric pressure, important deviations may appear between sets of data taken at higher pressures. Moreover, experimental information as a function of pressure is much less documented than studies as a function of temperature; even for very common chemical compounds, the data

[1] Laboratoire Haute Pression, Centre Universitaire de Recherche Scientifique, Université de Pau, Avenue de l'Université, 64000 Pau, France.
[2] To whom correspondence should be addressed.
[3] Laboratoire de Thermodynamique et Génie Chimique, UPRES A CNRS 6003, Université Blaise Pascal, 63177 Aubiere Cedex, France.

0195-928X/00/0700-0145$18.00/0

available still remain scarce. It is thus essential to measure such properties over extended pressure ranges and, in particular, to deduce pressure derivatives which are more directly related to molecular structures. In a recent thorough investigation of *n*-hexane, Randzio et al. [1] have carried out experimental determinations of isobaric thermal expansivities α_P over a wide range of temperature and pressure. These data, combined with other literature data, enabled them to develop numerically correlation equations from which several other thermodynamic properties such as densities ρ, isobaric and isochoric heat capacities (C_P and C_V), isothermal compressibilities κ_T, and thermal coefficients of pressure γ_B have been calculated for the entire range of pressure and temperature (i.e., from 240 to 523 K and up to 700 MPa). However, in that work, two properties were not considered: speed-of-sound and isentropic compressibility. The object of this paper consists primarily of supplementing the experimental database on *n*-hexane with speeds-of-sound measured at several pressures (0.1 to 150 MPa) and temperatures (293 to 373 K). Speed-of-sound data were then used for comparison with experimental values from the literature and with those calculated from the correlation of Randzio et al. [1] based on α_P and C_P measurements. The comparison was then extended to the properties deduced from the ultrasonic measurements, namely, the density ρ and the isentropic compressibility κ_S, as well as the isothermal compressibility κ_T.

2. EXPERIMENTAL

The velocity of propagation of ultrasonic waves in *n*-hexane was measured with a pulse transmission–reflection apparatus operating at 3 MHz. This frequency constitutes an acceptable compromise between lower frequencies, which give clear signals but reduce the precision, and higher frequencies, which permit a better precision of measurements but with a greater attenuation of the waves. The operation and calibration have been described in detail by Daridon [2]. Determination of the ultrasonic speeds results from a double measurement by direct chronometry of the transfer times of pulses by transmission and reflection within the cell containing the sample. The measuring cell is made up of a stainless-steel cylinder closed at both ends by two identical stainless-steel connecting bars, which are used as links between the piezoelectric transducers and the fluid sample. The dimensions of the cell were chosen from simulations of deformation in such a way as to minimize the mass of the cell, which involves thermal inertia, and to withstand pressures above 200 MPa. The length L of the sample path between the connecting bars, which is selected to obtain sufficient accuracy, depends on both temperature T and pressure P. The

effects of pressure and temperature are taken into account by the following relation:

$$L(P, T) = L_0[1 + a(T - T_0)] \cdot [1 + b(P - P_0)] \tag{1}$$

where $T_0 = 293.15$ K and $P_0 = 0.1$ MPa and where the coefficients a and b, which depend on the mechanical properties of materials composing the cell, were determined by calibrating with water. The reference data taken from literature were those of Wilson [3], Del Grosso et al. [4], and Petitet et al. [5].

In addition to the measuring cell, the overall experimental setup included various devices:

- an electric signal generator and a storage oscilloscope for the detection and analysis of the reflected and transmitted echoes;
- a double cylinder volumetric pump with a 50-MPa maximum pressure;
- a pressure multiplier, coupled with the volumetric pump to access much higher pressures (>200 MPa);
- a separator with a moving piston between the multiplier and the cell, whose role is to communicate the desired pressure to the fluid sample (avoiding direct contact between the pressure transmitting oil and the fluid sample); and
- an agitated bath thermoregulated by coupling air flow and heat-bearing oil.

3. RESULTS

n-Hexane was supplied by Sigma with a purity better than 99.9%. The ranges of temperature and pressure extended from 293.15 to 373.5 K and from 0.1 to 150 MPa, respectively, the steps adopted during the experiments being, respectively, 10 K and 5 MPa, so that the number of ultrasonic velocity measurements carried out on *n*-hexane was close to 300. For practical reasons, the determinations were conducted along nine isotherms, i.e., at a fixed temperature and variable pressure. Ultrasonic speeds measured in *n*-hexane are presented in Table I. The data were taken exclusively in the liquid state, which excludes values above 343 K at atmospheric pressure. Some isothermal curves as well as isobaric curves are plotted in Figs. 1 and 2. In agreement with the usual observation for the liquid state, these sets of curves show regular and smooth variations corresponding to positive pressure coefficients $(\partial u/\partial P)_T$ and negative temperature coefficients $(\partial u/\partial T)_P$.

Table I. Speed of Sound u in n-Hexane

	u (m·s^{-1}) at T (K)								
P (MPa)	293.15	303.15	313.15	323.15	333.15	343.15	353.15	363.15	373.15
0.1	1099.8	1054.6	1009.6	964.7	920.6				
5	1138.3	1095.9	1053.2	1011.1	969.7	929.2	888.7	849.2	809.4
10	1174.6	1134.1	1093.3	1054.1	1014.3	976.4	938.6	901.7	865.4
15	1208.8	1169.7	1131.1	1092.8	1055.3	1019.4	983.9	948.7	914.8
20	1241.1	1203.3	1165.8	1129.1	1093.4	1058.9	1024.9	991.6	959.2
25	1271.6	1234.7	1198.6	1163.4	1128.7	1095.4	1062.9	1031.2	1000.2
30	1300.8	1264.7	1230.0	1195.4	1162.3	1129.9	1098.6	1067.6	1038.3
35	1328.6	1293.6	1259.5	1225.8	1193.7	1162.4	1132.1	1102.5	1073.6
40	1354.8	1320.8	1287.7	1255.5	1223.8	1193.0	1163.4	1135.0	1106.8
45	1380.6	1346.9	1314.7	1282.7	1252.3	1222.5	1193.5	1165.7	1138.4
50	1405.0	1372.4	1340.2	1309.2	1279.8	1250.6	1222.1	1194.9	1168.7
55	1428.8	1396.8	1365.6	1335.4	1306.0	1277.3	1249.7	1223.5	1197.4
60	1451.8	1420.4	1389.8	1360.2	1330.9	1303.2	1276.0	1250.1	1224.5
65	1473.7	1443.1	1412.7	1383.5	1355.1	1328.0	1301.5	1275.7	1251.0
70	1495.5	1465.4	1435.9	1406.9	1378.6	1352.3	1326.2	1301.1	1276.6
75	1516.3	1486.6	1458.0	1429.2	1401.5	1375.2	1350.5	1325.1	1301.1
80	1536.8	1507.6	1478.8	1450.6	1423.6	1397.4	1372.6	1348.2	1324.5
85	1556.7	1527.8	1499.4	1471.7	1445.2	1419.4	1394.6	1370.7	1348.1
90	1575.8	1547.1	1519.7	1492.1	1465.9	1440.7	1416.5	1392.8	1369.8
95	1594.5	1566.5	1539.3	1512.3	1486.3	1461.3	1437.9	1414.2	1391.4
100	1613.5	1585.2	1558.2	1531.7	1506.2	1481.5	1458.1	1434.7	1412.5
105	1631.6	1603.6	1576.8	1550.6	1524.9	1500.9	1477.4	1454.7	1433.0
110	1648.8	1621.7	1595.0	1569.3	1544.3	1520.2	1497.1	1474.7	1452.6
115	1666.3	1639.4	1613.3	1587.6	1562.8	1538.9	1515.9	1494.1	1472.1
120	1683.4	1656.5	1630.6	1605.2	1580.9	1557.1	1534.7	1512.7	1491.2
125	1699.9	1673.2	1648.0	1622.3	1598.4	1575.4	1552.6	1530.6	1509.6
130	1716.0	1690.0	1664.7	1639.9	1615.8	1592.6	1570.3	1548.7	1527.8
135	1732.2	1706.4	1681.3	1656.4	1632.8	1609.9	1587.8	1566.3	1545.8
140	1747.6	1722.2	1697.7	1672.7	1649.4	1626.8	1604.9	1583.9	1563.3
145	1763.7	1737.8	1713.1	1688.9	1665.6	1643.3	1620.0	1600.9	1580.1
150	1778.1	1753.1	1728.8	1705.0	1681.4	1659.5	1636.6	1616.9	1596.8

The validity of the experimental method was checked by comparison with literature data available at atmospheric pressure as summarized in Table II. For this purpose, the literature data at $P = 0.1$ MPa were fitted with a cubic polynomial in temperature by using an objective function, with the experimental errors given for each data set taken into account. Values of the database deviating more than 0.5% from this function were

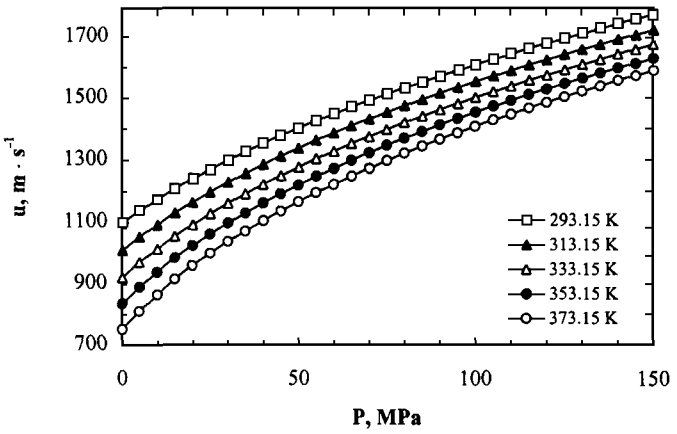

Fig. 1. Speed of sound u in n-hexane as a function of pressure.

deleted, and a larger weight was assigned to the more reliable measurements at 298.15 K. The optimum polynomial is

$$u(0.1\ \text{MPa}, T) = 3.4624 \times 10^3 - 1.4126 \times 10T + 2.9427 \times 10^{-2}T^2 - 2.9803 \times 10^{-5}T^3 \quad (2)$$

Our new values for n-hexane (not included in the fit) deviate from Eq. (2) by 0.035% on average (value of the average absolute deviation), with a

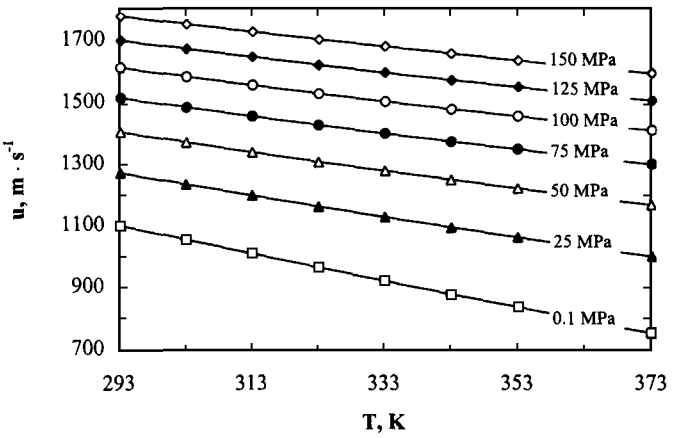

Fig. 2. Speed of sound u in n-hexane as a function of temperature.

Table II. References for Sound Speed in *n*-Hexane at Atmospheric Pressure

References	$T_{min} - T_{max}$ (K)	No. points
Aminabhavi and Gopalakrishna [13]	298.15	1
Benson and Handa [14]	298.15	1
Benson et al. [15]	298.15	1
Benson and Halpin [16]	298.15	1
Boelhouwer [6]	253.15–333.15	5
Handa et al. [17]	298.15	1
Junquera et al. [18]	298.15	1
Kagramanyan and Badalyan [8]	303.15–343.15	5
Kiryakov and Panin [7]	303.15–333.15	2
Sachdeva and Nanda [19]	293.15–333.15	6
Schaaffs and Shenoda [20]	298.15	1
Takagi and Teranishi [21]	298.15	1
Tardajos et al. [22]	298.15	1
Wang and Nur [23]	263.15–333.15	16

maximum deviation of 0.05%. This is lower than the experimental uncertainty estimated by Daridon [2] as 0.09%, including 0.03% due to the uncertainty in the temperature. It is worth mentioning that literature data show internal differences of more than 1%.

The speed-of-sound in *n*-hexane has been measured previously over a wide range of pressures and temperatures by several authors [6–8], whereas Yermakov et al. [9] have measured it at only moderate pressures but at high temperatures. Panin et al. [10] have determined the speed-of-sound as a function of density. The values provided by Boelhouwer [6], Kiryakov and Panin [7], and Kagramanyan and Badalyan [8] are, however, not mutually consistent, especially at higher pressures, with variations as high as 20 $m \cdot s^{-1}$, i.e., larger than 1%. Such significant differences between authors justified the present measurements to some extent. The comparison between our values and literature data at high pressures was done with different individual data sets. Comparison of our experimental data with those of Boelhouwer [6], over the range from 293 to 333 K and from 0.1 to 140 MPa, shows good agreement with an average absolute deviation of 0.083%. With Kiryakov and Panin [7] and Kagramanyan and Badalyan [8], the average absolute deviations from our results are, respectively, 0.79 and 0.81%. Finally, our measurements seem to be more coherent with those of Boelhouwer [6], while being located between those of Boelhouwer [6] and those of the two other authors.

4. DISCUSSION AND CORRELATION OF THE RESULTS

At frequencies of the order of a few megahertz, the ultrasonic speed u and the speed-of-sound C_0 extrapolated to zero frequency can be matched in the case of hydrocarbons in the liquid state. It follows from this assumption that the usual thermodynamic relations which relate the speed-of-sound to thermodynamic properties of the fluid can also be used for the ultrasonic speed. Thus, combination of the relations

$$u^2 = \left(\frac{\partial P}{\partial \rho}\right)_S = \frac{1}{\rho \kappa_S} \tag{3}$$

and

$$\kappa_S = \kappa_T - \frac{T\alpha_P^2}{\rho C_P} \tag{4}$$

where ρ, α_P, κ_S, κ_T, and C_P are, respectively, the density, the isobaric thermal expansivity, the isentropic and isothermal compressibilities, and the isobaric heat capacity, leads to the relation

$$\left(\frac{\partial \rho}{\partial P}\right)_T = \frac{1}{u^2} + \frac{T\alpha_P^2}{C_P} \tag{5}$$

which provides, by integrating with pressure, at a fixed temperature, the relationship

$$\rho(P, T) = \rho(P_0, T) + \int_{P_0}^{P} u^{-2}\, dP + T \int_{P_0}^{P} \frac{\alpha_P^2}{C_P}\, dP \tag{6}$$

where P_0 represents a reference pressure. This equation enables calculation of the density of the fluid under P, T conditions from a knowledge of its value as a function of temperature at the initial pressure P_0. The practical exploitation of this relationship, with a view to deduce densities at high pressures, requires the evaluation of the three terms on the right-hand side of Eq. (6). The first of them, $\rho(P_0, T)$, which represents the predominant contribution, is directly obtained from a measurement of ρ at the initial pressure P_0. In this work, the saturation pressures were used as reference pressures and the reference density was thus obtained from the correlation of the saturated volume as established by Randzio et al. [1]. The second term, whose contribution to the volume changes due to the pressure effects is much more significant than that from the third term, is evaluated directly through the knowledge of the speed-of-sound measured along various

isotherms. Evaluation of the third term can be made iteratively according to Davis and Gordon [11] by using the following additional thermodynamic relationships:

$$\left(\frac{\partial \alpha_P}{\partial P}\right)_T = -\left(\frac{\partial \kappa_T}{\partial T}\right)_P \tag{7}$$

$$\left(\frac{\partial C_P}{\partial P}\right)_T = -\frac{T}{\rho}\left\{\alpha_P^2 + \left(\frac{\partial \alpha_P}{\partial T}\right)_P\right\} \tag{8}$$

The method as a whole makes it possible to extend the determination of the density in the whole range of ultrasonic measurements, i.e., up to 150 MPa. However, to evaluate with good accuracy the integral of $1/u^2$, one needs to fit the values of $1/u^2$ using a function of pressure. In the same way, the iterative calculation of the last integral in Eq. (6) requires a small temperature step (less than 5 K and fixed at 1 K) to obtain good accuracy. This step, which is smaller than the experimental temperature step, requires interpolation of the speed-of-sound data at a given pressure by means of a smooth function of temperature. To meet these two requirements, a two-dimensional (P, T) function was used to interpolate the data of ultrasonic speed. A rational function was adopted to correlate directly $1/u^2$ instead of u:

$$\frac{1}{u^2} = \frac{A + BP + CP^2 + DP^3}{E + FP} \tag{9}$$

where

$$A = A_0 + A_1 T + A_2 T^2 + A_3 T^3 \tag{10}$$

and

$$E = 1 + E_1 T \tag{11}$$

This function, which needs only nine adjustable parameters (given in Table III), appeared to be well adapted to the experimental database (with an absolute average deviation of less than 0.02%). It offers, moreover, the advantage of leading to a simple analytical form of the integral of $1/u^2$:

$$\int u^{-2}\, dP = \left(\frac{B}{F} - \frac{CE}{F^2} + \frac{DE^2}{F^3}\right) P + \left(\frac{C}{F} - \frac{DE}{F^2}\right)\frac{P^2}{2} + \left(\frac{D}{F}\right)\frac{P^3}{3} + \left(\frac{A}{F} - \frac{BE}{F^2} + \frac{CE^2}{F^3} - \frac{DE^3}{F^4}\right)\ln(E + FP) \tag{12}$$

Table III. Parameters in Eq. (6) with T in K, P in MPa, and u in $m \cdot s^{-1}$

Parameters			Deviation of u
$A_0 = 2.34014 \times 10^{-7}$	$A_3 = -9.7804 \times 10^{-15}$	$D = 2.70706 \times 10^{-14}$	$AD\% = 4.5 \times 10^{-4}$
$A_1 = -1.21260 \times 10^{-9}$	$B = 2.65783 \times 10^{-9}$	$E_1 = -2.10375 \times 10^{-3}$	$AAD\% = 3.9 \times 10^{-2}$
$A_2 = 7.97759 \times 10^{-12}$	$C = -1.11830 \times 10^{-11}$	$F = 9.14581 \times 10^{-3}$	$MD\% = 1.4 \times 10^{-1}$

Table IV. Density ρ of *n*-Hexane Deduced from Ultrasonic Measurements

	ρ ($kg \cdot m^{-3}$) at T (K)								
P (MPa)	293.15	303.15	313.15	323.15	333.15	343.15	353.15	363.15	373.15
P_s	659.52	650.09	640.54	630.86	621.05	611.06	600.88	590.47	579.80
5	664.74	655.72	646.62	637.44	628.16	618.78	609.26	599.60	589.77
10	669.61	660.94	652.23	643.48	634.67	625.80	616.87	607.86	598.75
15	674.16	665.80	657.42	649.02	640.61	632.16	623.69	615.19	606.65
20	678.45	670.36	662.26	654.17	646.08	637.99	629.90	621.81	613.72
25	682.51	674.65	666.81	658.98	651.18	643.39	635.62	627.87	620.14
30	686.38	678.73	671.10	663.51	655.95	648.42	640.93	633.47	626.05
35	690.07	682.60	675.18	667.79	660.45	653.15	645.89	638.68	631.53
40	693.60	686.30	679.05	671.86	664.71	657.61	650.57	643.58	636.65
45	696.99	689.85	682.76	675.73	668.76	661.84	654.98	648.19	641.46
50	700.25	693.25	686.31	679.43	672.62	665.87	659.18	652.55	646.00
55	703.40	696.53	689.72	682.99	676.31	669.71	663.17	656.70	650.31
60	706.43	699.69	693.01	686.40	679.86	673.39	666.99	660.66	654.42
65	709.37	702.74	696.17	689.68	683.27	676.92	670.65	664.45	658.33
70	712.22	705.69	699.23	692.85	686.55	680.32	674.16	668.08	662.09
75	714.98	708.55	702.19	695.92	689.72	683.59	677.55	671.58	665.69
80	717.67	711.32	705.06	698.88	692.78	686.76	680.81	674.94	669.15
85	720.28	714.02	707.85	701.76	695.75	689.81	683.96	678.18	672.49
90	722.82	716.64	710.55	704.54	698.62	692.78	687.01	681.32	675.71
95	725.29	719.19	713.18	707.25	701.41	695.65	689.96	684.36	678.83
100	727.71	721.68	715.74	709.89	704.12	698.44	692.83	687.30	681.85
105	730.07	724.11	718.24	712.46	706.76	701.15	695.61	690.16	684.78
110	732.37	726.47	720.67	714.96	709.33	703.79	698.32	692.93	687.63
115	734.62	728.79	723.05	717.40	711.84	706.36	700.96	695.64	690.39
120	736.82	731.05	725.37	719.78	714.28	708.87	703.53	698.27	693.08
125	738.98	733.26	727.64	722.11	716.67	711.31	706.03	700.83	695.71
130	741.09	735.43	729.86	724.39	719.00	713.70	708.48	703.33	698.27
135	743.17	737.55	732.04	726.62	721.29	716.04	710.87	705.78	700.76
140	745.20	739.64	734.17	728.80	723.52	718.33	713.21	708.17	703.20
145	747.20	741.68	736.26	730.94	725.71	720.57	715.50	710.51	705.59
150	749.16	743.69	738.32	733.04	727.86	722.76	717.74	712.80	707.92

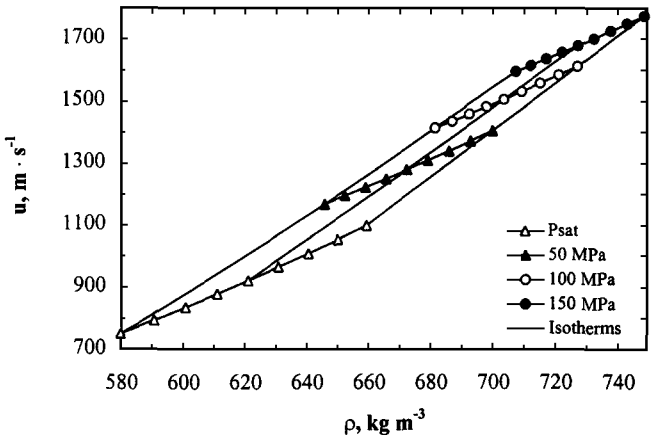

Fig. 3. Speed-of-sound u in n-hexane as a function of density ρ.

To avoid having to determine the derivative of κ_T, the effect of pressure on the thermal expansion coefficient is determined by a "predictor corrector" type approach rather than by using Eq. (7). This iterative approach consists, in a first stage, of predicting the density for $P + \Delta P$ from the knowledge of $\rho(P)$ with the quantity $T\alpha^2/C_P$ assumed to be constant [12]. The isobaric thermal expansivity $\alpha_P(T)$ for $P + \Delta P$ is then obtained by taking the derivative. The density calculated at the first stage is then corrected according to Eq. (6), in which α_P is interpolated linearly between the values known

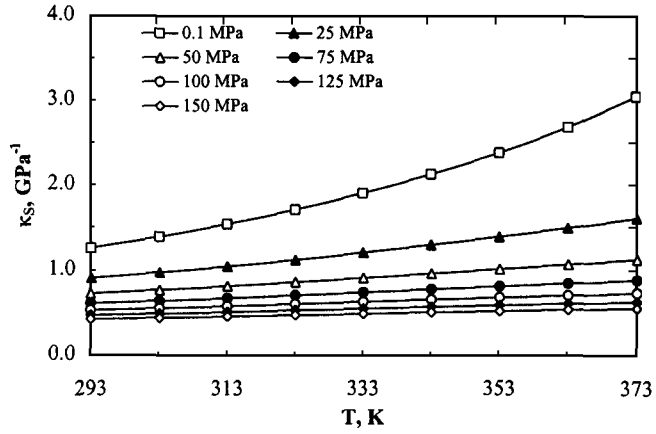

Fig. 4. Isentropic compressibility κ_S in n-hexane as a function of temperature.

at P and those predicted at $P+\Delta P$. This correcting step is repeated until $\rho(P+\Delta P)$ does not change. The isobaric heat capacity is then calculated at $P+\Delta P$ by means of Eq. (8) used in its integrated form.

Ultimately, this numerical procedure makes it possible to extend, from the reference pressure P_0 up to 150 MPa, the determination of the density of *n*-hexane from ultrasonic speed measurements. This approach requires a complementary knowledge of $\rho(T)$, $C_P(T)$, and $\alpha_P(T)$ as a function of T at the reference pressure only. In the present case, this additional information is given by the correlation of Randzio et al. [1] at the saturation

Table V. Isentropic Compressibility κ_S of *n*-Hexane

	κ_S (GPa^{-1}) at T (K)								
P (MPa)	293.15	303.15	313.15	323.15	333.15	343.15	353.15	363.15	373.15
P_s	1.2566	1.3883	1.5374	1.7070	1.9012	2.1251	2.3855	2.6915	3.0555
5	1.1610	1.2698	1.3942	1.5345	1.6929	1.8719	2.0783	2.3126	2.5879
10	1.0823	1.1763	1.2827	1.3987	1.5315	1.6761	1.8401	2.0236	2.2303
15	1.0152	1.0978	1.1890	1.2903	1.4017	1.5221	1.6561	1.8061	1.9699
20	0.9569	1.0302	1.1109	1.1991	1.2946	1.3980	1.5115	1.6356	1.7709
25	0.9062	0.9724	1.0438	1.1212	1.2055	1.2953	1.3925	1.4976	1.6119
30	0.8610	0.9211	0.9848	1.0547	1.1285	1.2079	1.2926	1.3850	1.4816
35	0.8209	0.8754	0.9336	0.9966	1.0626	1.1331	1.2081	1.2881	1.3738
40	0.7855	0.8353	0.8881	0.9442	1.0045	1.0684	1.1356	1.2062	1.2822
45	0.7527	0.7991	0.8473	0.8995	0.9535	1.0111	1.0718	1.1353	1.2029
50	0.7234	0.7659	0.8112	0.8586	0.9077	0.9603	1.0158	1.0734	1.1334
55	0.6964	0.7358	0.7775	0.8211	0.8669	0.9152	0.9655	1.0172	1.0726
60	0.6716	0.7084	0.7471	0.7874	0.8305	0.8744	0.9208	0.9686	1.0191
65	0.6491	0.6833	0.7198	0.7575	0.7970	0.8377	0.8803	0.9247	0.9706
70	0.6278	0.6599	0.6936	0.7292	0.7663	0.8038	0.8434	0.8841	0.9268
75	0.6084	0.6386	0.6700	0.7035	0.7382	0.7736	0.8092	0.8481	0.8874
80	0.5900	0.6185	0.6486	0.6800	0.7123	0.7456	0.7796	0.8151	0.8519
85	0.5729	0.6000	0.6284	0.6579	0.6881	0.7195	0.7518	0.7849	0.8182
90	0.5571	0.5830	0.6094	0.6375	0.6661	0.6955	0.7255	0.7566	0.7888
95	0.5423	0.5666	0.5918	0.6182	0.6454	0.6732	0.7010	0.7306	0.7609
100	0.5278	0.5514	0.5755	0.6004	0.6260	0.6524	0.6788	0.7069	0.7350
105	0.5145	0.5370	0.5600	0.5838	0.6085	0.6331	0.6586	0.6847	0.7112
110	0.5023	0.5234	0.5454	0.5680	0.5911	0.6149	0.6389	0.6636	0.6892
115	0.4902	0.5106	0.5314	0.5530	0.5752	0.5978	0.6208	0.6440	0.6684
120	0.4789	0.4985	0.5185	0.5392	0.5602	0.5818	0.6035	0.6259	0.6488
125	0.4683	0.4871	0.5060	0.5262	0.5461	0.5665	0.5875	0.6091	0.6307
130	0.4583	0.4761	0.4944	0.5133	0.5327	0.5524	0.5724	0.5928	0.6136
135	0.4485	0.4657	0.4832	0.5016	0.5200	0.5388	0.5580	0.5776	0.5972
140	0.4394	0.4559	0.4726	0.4904	0.5080	0.5260	0.5443	0.5629	0.5819
145	0.4302	0.4464	0.4628	0.4796	0.4967	0.5139	0.5325	0.5491	0.5676
150	0.4222	0.4375	0.4532	0.4693	0.4860	0.5024	0.5202	0.5366	0.5540

pressure P_S. Table IV contains the set of values of ρ provided by this numerical analysis. Combining u and ρ under the same conditions makes it possible to plot a group of curves $u(\rho)$ along isobars and isotherms (Fig. 3), the respective shapes of which are regular and almost linear. Moreover, the method yields the derived properties $\kappa_S(T, P)$, $\kappa_T(T, P)$ over the entire pressure and temperature ranges investigated (293 to 373 K and 0.1 to 150 MPa). The values obtained for these two properties are listed in Tables V and VI. The dependences of these thermomechanical coefficients on pressure and

Table VI. Isothermal Compressibility κ_T of *n*-Hexane

	κ_T (GPa^{-1}) at T (K)								
P (MPa)	293.15	303.15	313.15	323.15	333.15	343.15	353.15	363.15	373.15
P_s	1.6133	1.7840	1.9768	2.1956	2.4454	2.7326	3.0657	3.4562	3.9195
5	1.5165	1.6552	1.8097	1.9828	2.1776	2.3984	2.6503	2.9402	3.2771
10	1.4042	1.5220	1.6518	1.7950	1.9538	2.1304	2.3279	2.5498	2.8010
15	1.3100	1.4119	1.5229	1.6441	1.7767	1.9221	2.0821	2.2588	2.4548
20	1.2297	1.3189	1.4154	1.5197	1.6327	1.7551	1.8882	2.0330	2.1911
25	1.1603	1.2392	1.3241	1.4151	1.5129	1.6179	1.7308	1.8522	1.9831
30	1.0993	1.1700	1.2454	1.3258	1.4115	1.5029	1.6002	1.7040	1.8146
35	1.0454	1.1091	1.1767	1.2484	1.3244	1.4048	1.4899	1.5799	1.6750
40	0.9972	1.0550	1.1161	1.1806	1.2486	1.3201	1.3954	1.4744	1.5572
45	0.9538	1.0066	1.0622	1.1206	1.1819	1.2461	1.3132	1.3833	1.4564
50	0.9145	0.9629	1.0137	1.0670	1.1227	1.1807	1.2412	1.3039	1.3690
55	0.8786	0.9233	0.9700	1.0188	1.0697	1.1225	1.1773	1.2339	1.2924
60	0.8457	0.8871	0.9303	0.9752	1.0219	1.0703	1.1202	1.1717	1.2246
65	0.8155	0.8539	0.8939	0.9355	0.9786	1.0231	1.0689	1.1160	1.1642
70	0.7875	0.8233	0.8606	0.8992	0.9392	0.9803	1.0225	1.0657	1.1099
75	0.7615	0.7951	0.8299	0.8659	0.9030	0.9412	0.9803	1.0202	1.0608
80	0.7374	0.7688	0.8014	0.8351	0.8698	0.9053	0.9416	0.9787	1.0162
85	0.7149	0.7444	0.7751	0.8066	0.8391	0.8723	0.9062	0.9406	0.9755
90	0.6938	0.7217	0.7505	0.7802	0.8107	0.8418	0.8735	0.9057	0.9382
95	0.6741	0.7004	0.7276	0.7556	0.7843	0.8135	0.8433	0.8735	0.9039
100	0.6556	0.6805	0.7062	0.7326	0.7597	0.7873	0.8153	0.8437	0.8722
105	0.6381	0.6618	0.6861	0.7112	0.7368	0.7628	0.7893	0.8160	0.8428
110	0.6217	0.6442	0.6673	0.6911	0.7153	0.7400	0.7650	0.7902	0.8156
115	0.6063	0.6276	0.6496	0.6722	0.6952	0.7186	0.7423	0.7662	0.7902
120	0.5917	0.6120	0.6330	0.6545	0.6764	0.6986	0.7212	0.7438	0.7666
125	0.5779	0.5973	0.6173	0.6378	0.6587	0.6799	0.7013	0.7229	0.7445
130	0.5649	0.5835	0.6026	0.6221	0.6420	0.6623	0.6827	0.7032	0.7238
135	0.5526	0.5704	0.5886	0.6073	0.6264	0.6457	0.6652	0.6848	0.7044
140	0.5409	0.5580	0.5755	0.5934	0.6116	0.6301	0.6487	0.6675	0.6862
145	0.5299	0.5463	0.5630	0.5802	0.5977	0.6154	0.6333	0.6512	0.6691
150	0.5195	0.5352	0.5513	0.5678	0.5846	0.6016	0.6187	0.6359	0.6531

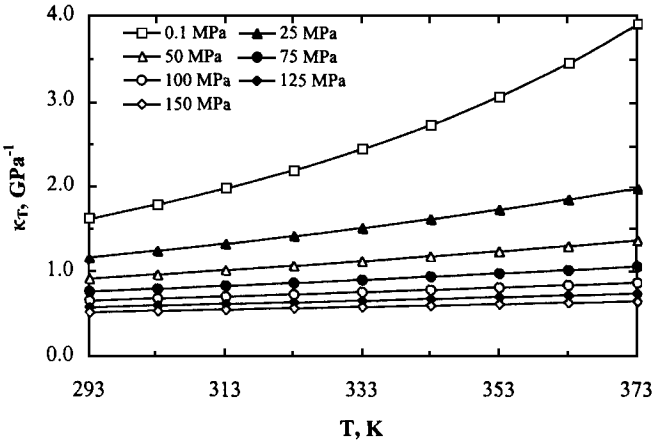

Fig. 5. Isothermal compressibility κ_T in *n*-hexane as a function of temperature.

temperature are illustrated in Figs. 4 and 5. These sets of curves are similar and simply shifted between each other by the $\alpha_P^2 T/\rho C_P$ term.

5. COMPARISONS AND THERMODYNAMIC CONSISTENCY

As shown in the preceding section, it is possible to generate, as a function of pressure, various thermophysical quantities of fluids from the values of speed-of-sound measured at several pressures and temperatures. It is one of the major interests of such experimental measurements. Evidently, it is also possible, by starting from the experimental measurements reported by Randzio et al. [1] and by using their correlation equations to get the speed-of-sound u and the isentropic compressibility κ_S according to the following relation

$$u = \left[\left(\frac{\partial \rho}{\partial P} \right)_T - \frac{T\alpha_P^2}{C_P} \right]^{-1/2} \tag{13}$$

To test the mutual consistency of both approaches and also to validate the numerical methods developed to generate some derived properties, the results obtained in the present work on *n*-hexane (i.e, u, ρ, κ_S, and κ_T) were compared with those of Randzio et al. [1] in the common range of the two investigations.

As for the speed-of-sound, the comparison of our experimental values with the values calculated from the correlation provided by Randzio et al.

[1], at the same P and T, reveals an average deviation (AD) of 0.0016% and an absolute average deviation (AAD) of 0.45%. This is a striking result taking into account the differences observed between the experimental determinations of different authors. Moreover, deviations are random. Finally, it can be noted from Fig. 6, which, for example, refers to a given temperature, that the deviations do not increase systematically with pressure. We therefore expect that the average uncertainty of about 0.5% will be preserved over the complete range of pressure [0.1 to 700 MPa] and thus that this kind of correlation is able to predict the behavior of this property up to very high pressures.

In the case of density, average absolute and average deviations of 0.072 and 0.043%, respectively, were observed. The comparison again reveals excellent agreement between the two sets of data, those resulting from measurements of the sound speed, on the one hand, and those resulting from measurements from the isobaric thermal expansivity, on the other hand.

A similar agreement can be observed between the densities calculated from the speed-of-sound measurements and the densities measured directly [24]. Values reported in standard reference data tables [24] and densities calculated from the speed-of-sound under the same conditions of temperature and pressure (290 to 370 K by steps of 10 K and up to 100 MPa) deviate by 0.02% on average with an average absolute deviation of 0.1%.

Similarly, the deviations obtained in the comparative study performed on the isentropic compressibility are −0.037 and 0.95% for the average

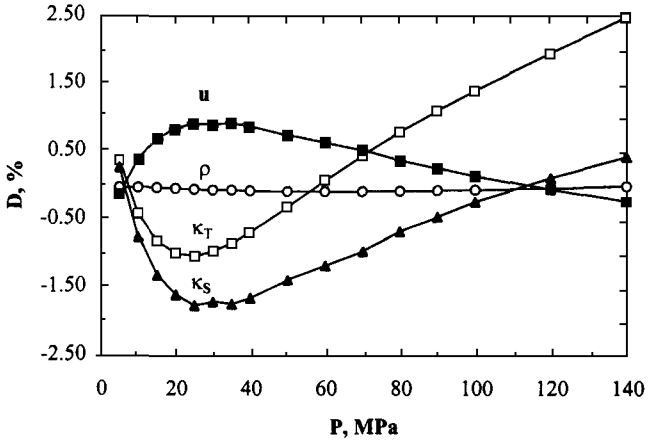

Fig. 6. Deviations (%) between the properties deduced from acoustic measurements and those calculated from the correlation of Randzio et al. [1].

and the average absolute deviations, respectively. These variations increase up to 1.29 and 1.42% in the case of the isothermal compressibility κ_T. The deviations observed for κ_S and κ_T result primarily from the uncertainties of the respective derivatives $(\partial\rho/\partial P)_S$ and $(\partial\rho/\partial P)_T$. These deviations are divided by two in sound speed, which is explained by the fact that u is related to κ_S by

$$\kappa_S = \frac{1}{\rho u^2} \tag{14}$$

Thus $\sigma u/u$ differs little from 1/2 $(\sigma\kappa_S/\kappa_S)$, since $\sigma\rho/\rho$ is lower. The comparison made for the coefficients of compressibility can also be considered as satisfactory; the deviations between our values and those of Randzio et al. [1] are within $\pm 1\%$, which is satisfactory. The deviations plotted in Fig. 6 for a given temperature give a precise idea of how the deviations depend on pressure.

6. CONCLUSION

Ultrasonic velocity measurements carried out on *n*-hexane between 0.1 and 150 MPa and 293 and 373 K were used to generate the density as well as its derivatives κ_S and κ_T as a function of pressure. The results obtained made it possible to check the overall consistency between our values and those calculated from the thermodynamic model developed by Randzio et al. [1]. The very satisfactory agreement observed between the two methods in this pressure range as well as the absence of systematic deviations indicates that the thermophysical behavior of *n*-hexane and, in particular, its derived properties as a function of pressure are well described by the correlation equations of Randzio et al. [1]. Good agreement of the densities calculated from the speed-of-sound measurements with the densities measured directly confirm the good quality of both the experimental measurements and the correlating relationships.

REFERENCES

1. S. L. Randzio, J.-P. E. Grolier, J. R. Quint, D. J. Eatough, E. A. Lewis, and L. D. Hansen, *Int. J. Thermophys.* **15**:415 (1994).
2. J. L. Daridon, *Acoustica* **80**:416 (1994).
3. W. D. Wilson, *J. Acoust. Soc. Am.* **31**:1067 (1959).
4. V. A. Del Grosso and C. W. Mader, *J. Acoust. Soc. Am.* **52**:1442 (1972).
5. J. P. Petitet, R. Tufeu, and B. Le Neindre, *Int. J. Thermophys.* **4**:35 (1983).
6. J. W. M. Boelhouwer, *Physica* **34**:484 (1967).
7. B. S. Kiryakov and P. P. Panin, *Nauk. Tr. Kursk. Gos Pedagog. Inst.* **7**:132 (1972).

8. L. S. Kagramanyan and A. L. Badalyan, *Izv. Akad. Nauk. Arm. USSR Fiz.* **13**:478 (1978)
9. G. V. Yermakov and R. G. Ismagilov, *Heat Trans. Sov. Res.* **11**:47 (1979)
10. P. P. Panin, *Nauk. Tr. Kursk. Gos. Pedagog. Inst.* 7:26 (1972).
11. L. A. Davis and R. B. Gordon, *J. Chem. Phys.* **46**:2650 (1967).
12. L. Denielou, J. P. Petitet, C. Tequi, and G. Syfosse, *Bull. Minéral.* **106**:139 (1983).
13. T. M. Aminabhavi and B. Gopalakrishna, *J. Chem. Eng. Data* **40**:632 (1995).
14. G. C. Benson and Y. P. Handa, *J. Chem. Thermodyn.* **13**:887 (1981).
15. G. C. Benson, C. J. Halpin, and M. K. Kumaran, *J. Chem. Thermodyn.* **18**:1147 (1986).
16. G. C. Benson and C. J. Halpin, *Can. J. Chem.* **65**:322 (1987).
17. Y. P. Handa, C. J. Halpin, and G. C. Benson, *J. Chem. Thermodyn.* **13**:875 (1981).
18. E. Junquera, G. Tardajos, and E. Aicart, *J. Chem. Thermodyn.* **20**:1461 (1988).
19. V. K. Sachdeva and V. S. Nanda, *J. Chem. Phys.* **75**:4745 (1981).
20. V. W. Schaaffs and F. B. Shenoda, *Acoustica* **21**:366 (1969).
21. T. Takagi and H. Teranishi, *Fluid Phase Equil.* **20**:315 (1985).
22. G. Tardajos, M. Diaz Pena, and E. Aicart, *J. Chem. Thermodyn.* **18**:683 (1986).
23. Z. Wang and A. Nur, *J. Acoust. Soc. Am.* **89**:2725 (1991).
24. *Tables of Standard Reference Data, n-hexane, GSSSD 90-85* (USSR State Committee on Standards, Moscow, 1986).